The thermal decomposition of copper(II) oxalate revisited

Emmanuel Lamprecht, Gareth M. Watkins and Michael E. Brown

Abstract

DSC, TG and TG-FT-IR, and XRPD have been used to examine the effects of supposedly inert atmospheres of argon and nitrogen on the mechanism of the thermal decomposition of copper(II) oxalate. The DSC curves in pure argon at 10 °C min^{-1} show a broad endotherm with onset at about 280 °C and maximum at about 295 °C. In mixtures of argon and nitrogen, as the proportion of argon gas is decreased, the endothermic character of the decomposition decreases until, when nitrogen is the main component, the decomposition exhibits a complex broad exothermic character. XRPD studies showed that, regardless of the proportions of nitrogen and argon, the DSC residues consisted of mainly copper metal with small amounts of copper(I) oxide (cuprite) and, under some conditions, traces of copper(II) oxide (tenorite). Various explanations for this behaviour are discussed and a possible answer lies in the disproportionation of $CO_2(g)$ to form small quantities of $O_2(g)$ or monatomic oxygen. The possibility exists that the exothermicity in nitrogen could be explained by reaction of the nitrogen with atomic oxygen to form $N_2O(g)$, but this product could not be detected using TG-FT-IR.

1. Introduction

Some anomalies in the thermal behaviour of other copper(II) carboxylate complexes [1] indicated a need to re-examine some aspects of the thermal decomposition of copper(II) oxalate, which is reported to be an exothermic process under nitrogen purge [2], [3] and [4], in a self-generated atmosphere [5], and in various atmospheres including hydrogen and carbon dioxide[6]. Decomposition may take place by various pathways [7] and [8], of which the three main competing reactions are:

$$CuC_2O_4(s):\ a \rightarrow Cu(s) + 2CO_2(g);\ b \rightarrow (1/2)Cu_2O(s) + (1/2)CO(g) + 1(1/2)CO_2(g);\ c \rightarrow CuO(s) + CO(g) + CO_2(g) \quad (1)$$

The overall chemical equation is then:

$$\alpha + \beta + \gamma)CuC_2O_4(s) \rightarrow \alpha Cu(s) + 2\alpha CO_2(g) + (1/2)\beta Cu_2O(s) + (1/2)\beta CO_2(g) + \gamma CuO(s) + \gamma CO(g) + \gamma CO_2(g) \quad (2)$$

where $\alpha + \beta + \gamma = 1$. We may substitute for α using $\alpha = 1 - \beta - \gamma$ so that Eq. (2) becomes:

$$CuC_2O_4(s) \rightarrow (1 - \beta - \gamma)Cu(s) + 2(1 - \beta - \gamma)CO_2(g) + (1/2)\beta Cu_2O(s) + (1/2)\beta CO(g) + 1(1/2)\beta CO_2(g) + \gamma CuO(s) + \gamma CO(g) + \gamma CO_2(g) \quad (3)$$

This may be simplified to:

$$CuC_2O_4(s) \rightarrow (1 - \beta - \gamma)Cu(s) + (1/2)\beta Cu_2O(s) + \gamma CuO(s) + ((1/2)\beta + \gamma)CO(g) + (2 - (1/2)\beta - \gamma)CO_2(g) \quad (4)$$

in which β is the fraction of the available copper(II) oxalate that undergoes decomposition via process *b*, and γ is the fraction that undergoes decomposition via process *c*. Individually, $0 \leq \beta \leq 1$ and $0 \leq \gamma \leq 1$, and together $\beta + \gamma \leq 1$.

An expression for the standard enthalpy change for reaction (3) can be written as a function of β and γ:

$$\Delta_r H°(\beta, \gamma) = (1/2)\beta\Delta_f H°Cu_2O(s) + \gamma\Delta_f H°CuO(s) + ((1/2)\beta + \gamma)\Delta_f H°CO(g) + (2 - (1/2)\beta - \gamma)\Delta_f H°CO_2(g) - \Delta_f H°CuC_2O_4(s) \quad (5)$$

Using standard values for the enthalpies of formation of $Cu_2O(s)$, $CuO(s)$, $CO(g)$ and $CO_2(g)$ [9] and a published value [10] of −751.3 kJ mol^{-1} for $\Delta_f H°CuC_2O_4(s)$, this may be written numerically as

$$\Delta_r H°(\beta, \gamma)\ (\text{kJ mol}^{-1}) = 58.13\beta + 127.72\gamma - 35.56 \quad (6)$$

If it is assumed that only path *a* is followed, i.e. that no oxidation takes place via paths *b* and *c*, then $\Delta_r H°$ ($\beta = 0$, $\gamma = 0$) (kJ mol^{-1}) = − 35.56. If it assumed that complete oxidation takes place via paths *b* and *c*, then $\beta + \gamma = 1$, and substitution of $\beta = 1 - \gamma$ in Eq. (6) gives:

$$\Delta_r H°(\gamma)\ (\text{kJ mol}^{-1}) = 69.59\gamma + 22.57 \quad (7)$$

Thus, if complete oxidation takes place via path b only (i.e. $\gamma = 0$), then $\Delta_r H°$ ($\gamma = 0$) (kJ mol^{-1}) = 22.57 and if complete oxidation takes place via path *c* only (i.e. $\gamma = 1$), then $\Delta_r H°$ ($\gamma = 1$) (kJ mol^{-1}) = 92.16. So the DSC response for this reaction can be exothermic or endothermic, depending on β and γ. The most exothermic DSC response possible is −35.56 kJ mol^{-1} and the most endothermic response possible is 92.16 kJ mol^{-1}.

If only processes *a* and *b* take place (i.e. $\gamma = 0$), then Eq. (4) becomes:

$$CuC_2O_4(s) \rightarrow (1 - \beta)Cu(s) + (1/2)\beta Cu_2O(s) + (1/2)\beta CO(g) + (2 - (1/2)\beta)CO_2(g) \quad (8)$$

and by setting $\gamma = 0$ in Eq. (6):

$$\Delta_r H°(\beta)\ (\text{kJ mol}^{-1}) = 58.13\beta - 35.56 \quad (9)$$

and $-35.56 \leq \Delta_r H°(\beta)\ (\text{kJ mol}^{-1}) \leq +22.57$.

If only processes *a* and *c* take place (i.e. $\beta = 0$), then Eq. (4) becomes:

$$CuC_2O_4(s) \rightarrow (1 - \gamma)Cu(s) + \gamma CuO(s) + \gamma CO(g) + (2 - \gamma)CO_2(g) \quad (10)$$

and Eq. (6) becomes

$$\Delta_r H°(\gamma)\ (\text{kJ mol}^{-1}) = 127.72\gamma - 35.56 \quad (11)$$

and $-35.56 \leq \Delta_r H°(\gamma)\ (\text{kJ mol}^{-1}) \leq +92.16$.

The oxalates of nickel, manganese, silver, mercury and lead have been proposed [11] to decompose by a mechanism of dissociative evaporation, i.e. by the simultaneous gasification of all reaction products irrespective of their volatility, and subsequent condensation of low-volatility species [12], [13], [14] and [15]. The decompositions of silver(I), nickel(II) and mercury(II) oxalate are said to be accompanied by the evolution of $CO(g)$, $CO_2(g)$ and $(1/2)O_2(g)$ or $O(g)$. The consequences of such a mechanism are considered in the discussion of results.

2. Experimental

2.1. Preparation and characterization

Copper(II) oxalate was prepared [3] by precipitation from aqueous solutions of copper(II) sulfate (0.20 mol L^{-1}) and potassium oxalate (0.13 mol L^{-1}). The product was dried in air at 120 °C for 5 days prior to use. The calculated formulae from analytical data for the dried and undried material are CuC_2O_4, $0.02H_2O$ and CuC_2O_4, $0.1H_2O$, respectively.

The X-ray powder diffraction patterns, using nickel-filtered Cu Kα radiation, for the undried and dried copper(II) oxalate are shown in Fig. 1. No observable structural changes occurred as a result of drying.

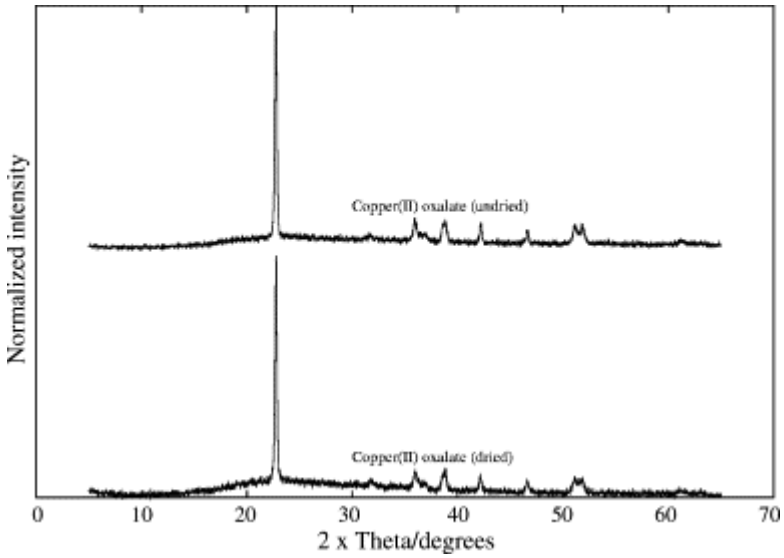

Fig. 1. X-ray powder diffraction patterns, using nickel-filtered Cu Kα radiation, for undried and dried copper(II) oxalate.

The infrared spectra of both the undried and dried copper(II) oxalate samples in KBr pellets compared well with the spectrum reported in the literature [3].

2.2. Thermal analysis equipment

Samples of copper(II) oxalate were examined using a Perkin-Elmer 7-Series differential scanning calorimeter (DSC) and thermogravimetric analyzer (TG) coupled with evolved gas analysis (EGA) by FT-IR. The DSC was calibrated for temperature using the melting points of indium metal and zinc metal, and for heat-flow using the standard enthalpy of fusion of indium metal. These calibrations were performed under argon purge, and measurements with the same calibrants under nitrogen were practically unchanged. The TG was calibrated for temperature under argon purge using the Curie points of Perkalloy and zinc.

Samples were heated in the DSC, in crimped (but not sealed) aluminium pans, from 25 to 350 °C in argon, nitrogen, mixed nitrogen–argon, and oxygen atmospheres at various heating rates (10, 5 and 2 °C min^{-1}) and purge flow rates (15–25 mL min^{-1}). The specifications of the nitrogen used stated maximum impurities in vpm of 3 for oxygen and for water and 2 for CO_2 + CO. The figures for the argon used were slightly lower at 2 for oxygen and for water, 6 for nitrogen and 2 for CO_2 + CO. Some experiments were done under argon and nitrogen using sealed pans perforated by a single pin-prick.

The mixed atmospheres were generated by means of a needle-valve system. The TG and the DSC were purged for several hours at every change of atmosphere, and purged for at least 15 min after each sample change before applying the temperature programme. The TG furnace tube was kept under a positive pressure of the atmosphere in use to minimize interference from residual air. A 15 ppb oxygen/moisture/hydrocarbon trap in tandem with an indicating trap did not alter the observed behaviour.

To ensure that the DSC furnace was purging correctly, the reference furnace was blocked with a strip of adhesive tape and the flow rate through the sample furnace checked at the common exhaust line. The procedure was then repeated with the sample furnace blocked and the reference furnace open. The sample and reference furnaces were both found to be purging normally.

The TG exhaust line was interfaced to an FT-IR gas cell fitted to a Perkin-Elmer FT-IR-2000 spectrometer. To test whether the evolution of carbon monoxide could be detected in the purge gas in the presence of the exposed platinum parts of the furnace, a sample of nickel squarate [16] was decomposed in argon. A weak IR absorption was observed in the carbon monoxide region (doublet-envelope centred at 2143 cm^{-1} [17]).

3. Results

3.1. TG-FT-IR results in inert atmospheres

The TG curves for copper(II) oxalate heated from 25 to 315 °C at 10 °C min^{-1} under argon and nitrogen atmospheres are given in Fig. 2. The curves are practically identical within the limits of sample-to-sample repeatability, showing a slow mass-loss of approximately 0.8% between 25 and 264 °C, followed by rapid decomposition between 264 and 310 °C. Residues heated beyond 320 °C showed a marked mass gain, probably due to oxidation by traces of residual air in the furnace.

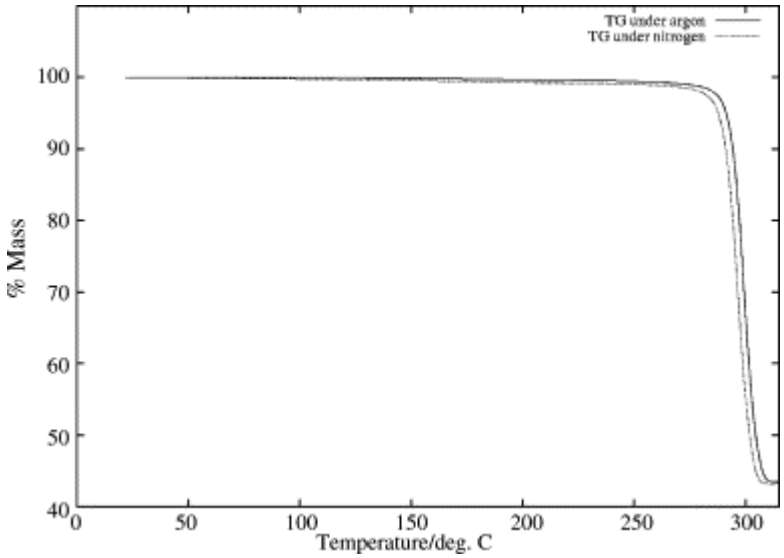

Fig. 2. The TG curves for copper(II) oxalate heated from 25 to 315 °C at 10 °C min^{-1} under argon and nitrogen atmospheres.

The residues under argon and nitrogen at 315 °C account, respectively, for 43.5% and 43.2% of the original sample masses. By comparison, the calculated mass percentage of copper in the dried copper oxalate is 41.84%. It is clear, therefore, that some oxidation of the copper in the samples has taken place, by residual air in the TG, by disproportionation of carbon dioxide, or both. The X-ray powder diffraction patterns of the TG residues confirmed that some oxidation to Cu (I) oxide had taken place under both argon and nitrogen atmospheres.

Residual air in TG furnaces can be extremely difficult [18] to remove effectively because of less than ideal design characteristics of their purging arrangements. This is particularly true of a Perkin-Elmer TG furnace that has been modified for interfacing to an FT-IR gas cell. These modifications are mentioned in the manufacturer's on-line catalogue [19] and similar modifications are described in more detail in the open literature [20]. Substances that are very sensitive to oxidation, such as finely divided metal powders, including the residues from the decomposition of copper(II) oxalate [18] have been suggested as diagnostic tools for checking purging efficiency.

The formation of copper(I) oxide through the disproportionation of carbon dioxide must result in the evolution of carbon monoxide. Three-dimensional plots of the evolved gas analysis data for TG runs under argon and nitrogen are shown in Fig. 3 and Fig. 4, respectively. The *Y*-axes are labelled with the TG programme temperature as calculated from the run-time. Under both argon and nitrogen atmospheres, the main decomposition step (beginning at about 270 °C) is accompanied by the release of carbon dioxide (expected CO_2 anti-symmetric stretch at 2349 cm^{-1} and CO_2 bend at 667 cm^{-1} [17]) and water (marked increase in the water symmetric stretch at 3652 cm^{-1} [17]). In addition, a very slight disturbance in the base-plane at about (2200 cm^{-1}, 300 °C) is observable in the runs under both argon and nitrogen. Greatly magnified spectrum slices in this temperature region (not illustrated) exhibit the fundamental carbon monoxide absorption (doublet-envelope centred at 2143 cm^{-1} [17]).

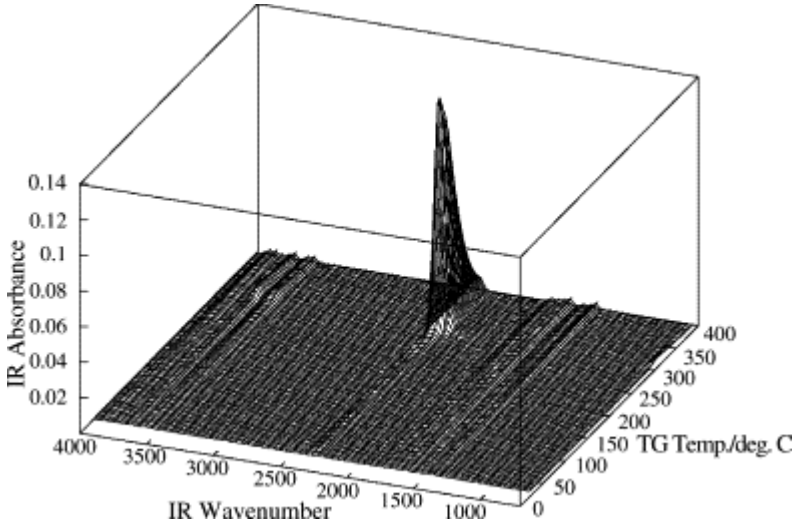

Fig. 3. TG-FT-IR evolved gas analysis results for copper(II) oxalate heated in argon from 25 to 315 °C at 10 °C min^{-1}. The interval from 315 to 400 °C is plotted only because of a time-lag between the TG and IR responses. Linear IR wavenumber scale.

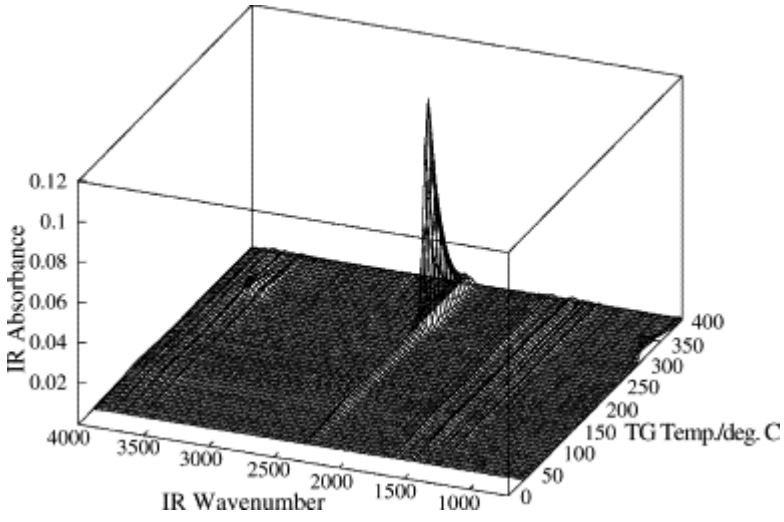

Fig. 4. TG-FT-IR evolved gas analysis results for copper(II) oxalate heated in nitrogen from 25 to 315 °C at 10 °C min^{-1}. The interval from 315 to 400 °C is plotted only because of a time-lag between the TG and IR responses. Linear IR wavenumber scale.

A considerable dead volume exists between the TG furnace and the FT-IR gas-cell, so a substantial broadening of the FT-IR absorbance signals along the time-axis is to be expected, and a time-delay of approximately 2 min exists between the appearance of a thermal event in the TG signal and the event being observed at the spectrometer. The large platinum surfaces in the TG furnace may also promote catalytic conversion of carbon monoxide to carbon dioxide in the presence of residual air.

3.2. DSC results in oxygen

A sample of dried copper(II) oxalate heated in the DSC under oxygen from 25 to 350 °C at 10 °C min^{-1} (see Fig. 5) gave a strong exotherm in two incompletely resolved stages with onset at about 250 °C and maximum at about 307 °C. The residue was identified by X-ray powder diffraction as CuO (tenorite) with no discernable trace of Cu_2O (cuprite) or copper metal. The X-ray diffraction pattern is very weak, indicating poor crystallinity of the residue. The residue also readily adsorbed water from the atmosphere. Table 1 summarizes the DSC results in oxygen.

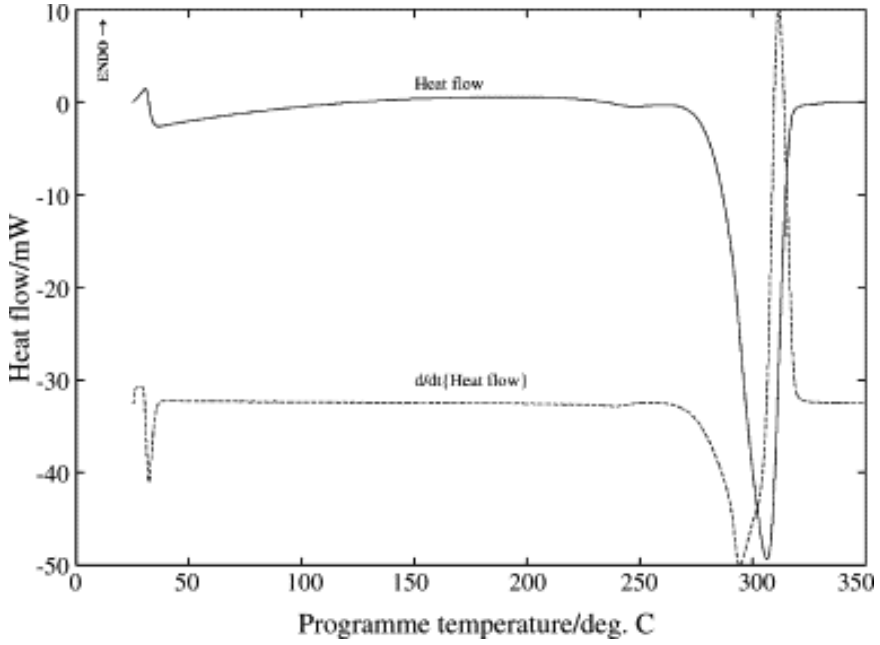

Fig. 5. DSC and derivative DSC curves of copper(II) oxalate heated in oxygen from 25 to 350 °C at 10 °C min^{-1}. The derivative curve was smoothed by means of a simple 11-point boxcar algorithm.

Table 1.

The DSC results for copper(II) oxalate heated in oxygen from 25 to 350 °C at 10 °C min^{-1}

Sample mass, m_s (mg)	4.913	5.449
Residual mass, m_r (mg)	2.582	2.843
$100m_s/m_r$	52.55	52.17
Q (J g^{-1})	−1470	−1475
$\Delta_r H$ (kJ mol^{-1})	−223.3	−224.0

Assuming the oxidation reaction:

$$CuC_2O_4(s) + 0.5O_2(g) \rightarrow CuO(s) + 2CO_2(g)$$

the enthalpy of formation of copper(II) oxalate is given by:

$$\Delta_f H°CuC_2O_4(s) = -\Delta_r H° + \Delta_f H°CuO(s) + 2\Delta_f H°CO_2(g)$$

Taking the integrated exothermic DSC response as $\Delta_r H°$ and substituting standard values for $\Delta_f H°CuO(s)$ and $\Delta_f H°CO_2(g)$ [9] gives $\Delta_f H°CuC_2O_4(s) = -718.3$ kJ mol^{-1}. This is approximately 5% below Le Van's published value of −751 kJ mol^{-1} [10].

3.3. DSC results in inert atmospheres

The DSC curves for copper oxalate heated in argon, nitrogen and mixed argon–nitrogen atmospheres are shown in Fig. 6. In pure argon there is a broad endotherm with onset at about 280 °C and a shoulder at about 293 °C reaching a maximum at about 295 °C. As the proportion of argon in the purge gas is decreased, the endothermic character of the decomposition decreases until, when nitrogen is the main component, the decomposition exhibits a broad exothermic character. The derivative DSC curves in Fig. 7, illustrate the complexity of the endothermic decompositions under pure argon and mainly argon atmospheres. At least four poorly resolved stages are apparent. The exotherms are also complex, showing at least two steps. The complexity of the endotherms under argon suggests some contribution from an exothermic process that is dominant under mainly nitrogen and pure nitrogen atmospheres.

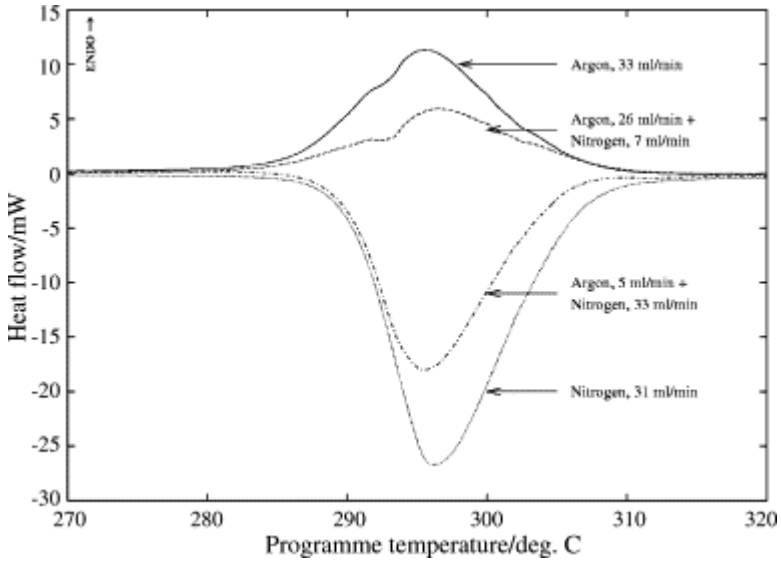

Fig. 6. DSC curves of copper(II) oxalate, heated in crimped aluminium pans, in various mixed argon–nitrogen atmospheres from 25 to 350 °C at 10 °C min^{-1}. Samples were of similar masses (4 mg). Baseline correction was performed by simple linear subtraction.

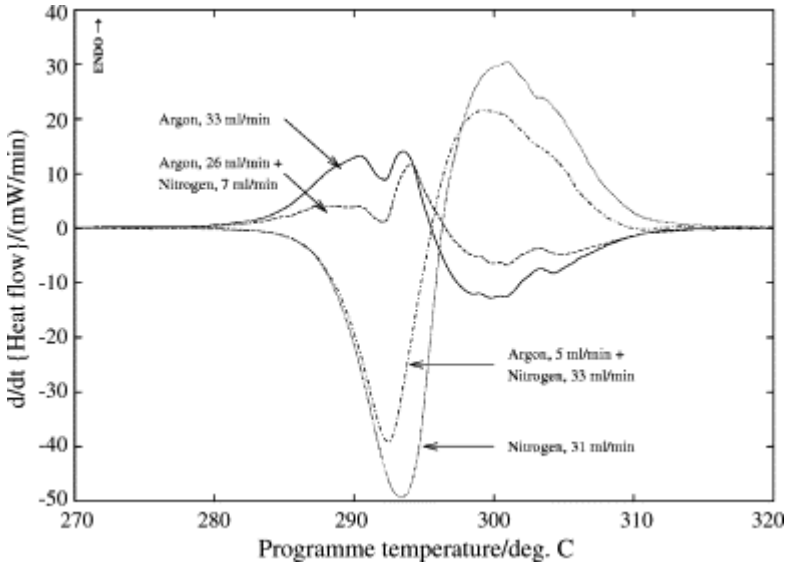

Fig. 7. Derivative DSC curves of copper(II) oxalate (see Fig. 6), heated in crimped aluminium pans, in various mixed argon–nitrogen atmospheres from 25 to 350 °C at 10 °C min^{-1}. Samples were of similar masses (4 mg). The derivatives were smoothed using a simple 11-point boxcar algorithm.

XRPD studies showed that, regardless of the proportions of nitrogen and argon, the DSC residues consisted of mainly copper metal with small amounts of copper(I) oxide (cuprite) and no discernable traces of copper(II) oxide (tenorite). The possibility that some oxidation of the residues took place during handling could not be excluded.

Table 2 and Table 3 summarize the mass and thermochemical data obtained from these DSC runs. The average percentages of the original sample masses (m_s) that the masses of the residues (m_r) constitute do not vary significantly from one inert atmosphere to the next. The calculated mass percentage of copper in the dried copper(II) oxalate is 41.84%, which is very close to the experimental values of $100m_r/m_s$.

Table 2.

DSC results for copper(II) oxalate heated (a) in crimped aluminium pans, and (b) in sealed but pierced pans, under 100% argon and 100% nitrogen atmospheres at flow rates of 32 ± 1 mL min^{-1}

	100% Argon	100% Nitrogen
(a) Crimped pans		
Average residual mass (%)	41.9 ± 0.2	41.8 ± 0.2
Average Q (J g^{-1})	187 ± 10	−398 ± 10
Average $\Delta_r H$ (kJ mol^{-1})	28.4 ± 1.5	−60.4 ± 1.5
(b) Sealed but pierced pans		
Average residual mass (%)	41.6 ± 0.3	41.6 ± 0.1
Average Q (J g^{-1})	307 ± 50	−415 ± 13
Average $\Delta_r H$ (kJ mol^{-1})	47 ± 8	−63 ± 2

Table 3.

DSC results for copper(II) oxalate heated in crimped aluminium pans under mixed argon-nitrogen atmospheres

	Argon (26 mL min^{-1}) and nitrogen (7 mL min^{-1})	Argon (5 mL min^{-1}) and nitrogen (33 mL min^{-1})
Average residual mass (%)	41.92 ± 0.20	41.75 ± 0.20
Average Q (J g^{-1})	110 ± 3	−257 ± 20
Average $\Delta_r H$ (kJ mol^{-1})	16.8 ± 0.5	−39 ± 3

From the XRPD and mass data, there is no significant difference in the extent of oxidation to Cu_2O of the samples from one inert atmosphere to the next. There is thus no evidence from the solid residues to suggest that different reactions are taking place under the four different inert atmospheres.

3.4. Decomposition in a self-generated atmosphere

Some samples were heated in sealed cold-welded pans with the lids perforated by a single pin-prick to allow the evolved gases to escape slowly under pressure, thus surrounding the decomposing samples with their own self-generated atmosphere. The results were similar to those with crimped (unsealed) pans but not as self-consistent. Under argon purge, an endothermic decomposition was observed, whereas under nitrogen an exotherm was obtained. The residue mass percentages still corresponded well to the calculated mass-percentage of copper, 41.84%. The average thermochemical data for the runs under nitrogen are very close to those obtained using crimped pans, but the average enthalpy of decomposition under argon is about 1.6 times greater.

3.5. DSC results at various heating rates

Fig. 8 shows the DSC curves for copper(II) oxalate heated under argon (25 mL min^{-1}) from 25 to 360 °C at 10, 5 and 2 °C min^{-1}. In addition to the expected shift towards lower temperatures in the onset, peak and end temperatures resulting from the different heating rates, the DSC curves appear more complex as the heating rate is decreased. At 10 °C min^{-1} (curve a), the left-hand lobe of the derivative DSC curve shows only one step, whereas the right-hand lobe shows two overlapping steps. In curve b (5 °C min^{-1}), there is a shoulder on the left-hand lobe, and clearer resolution of the two steps in the right-hand lobe. Curve c (2 °C min^{-1}) shows two incompletely resolved steps and the right-hand lobe shows further separation of the two steps observed in A and B.

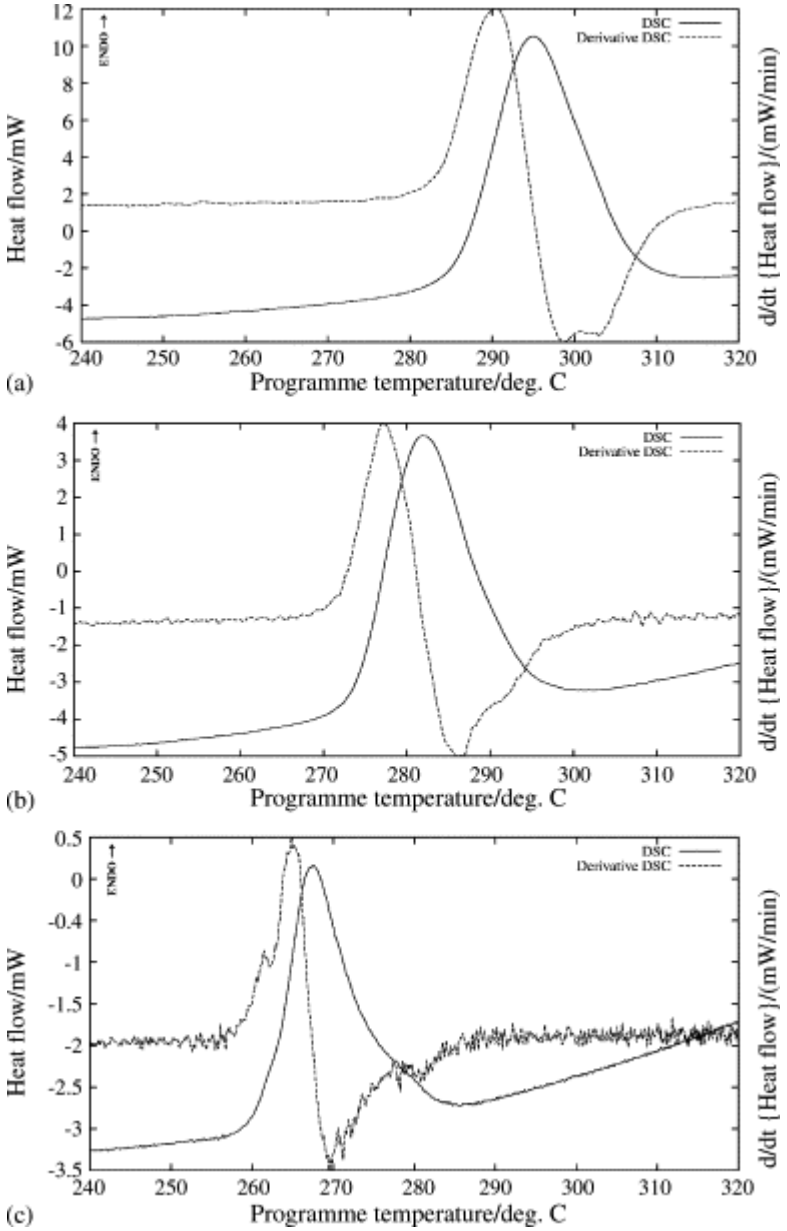

Fig. 8. DSC curves for copper(II) oxalate heated under argon (25 mL min^{-1}) from 25 to 360 °C at: (a) 10 °C min^{-1}; (b) 5 °C min^{-1}; (c) 2 °C min^{-1}.

The X-ray powder diffraction patterns of the DSC residues show that the residue of the 10 °C min^{-1} run consists of a mixture of copper metal and copper(I) oxide (cuprite), with no detectable copper(II) oxide (tenorite). At the slower heating rates, some copper(II) oxide formation is observed.

Fig. 9 shows DSC curves for copper(II) oxalate heated under nitrogen (24 mL min^{-1}) from 25 to 360 °C at 10, 5 and 2 °C min^{-1}. The left-hand lobes of the derivative DSC curves are all clearly single, but as under argon purge, the right-hand lobes show two steps becoming more clearly separated at lower heating rates. The X-ray powder diffraction patterns of the DSC residues under nitrogen follow the same trend as those under argon. The residue at 10 °C min^{-1} consists of a mixture of copper metal and copper(I) oxide (cuprite) with no detectable copper(II) oxide (tenorite), but the magnitude of the tenorite peaks increases as the DSC heating rate decreases.

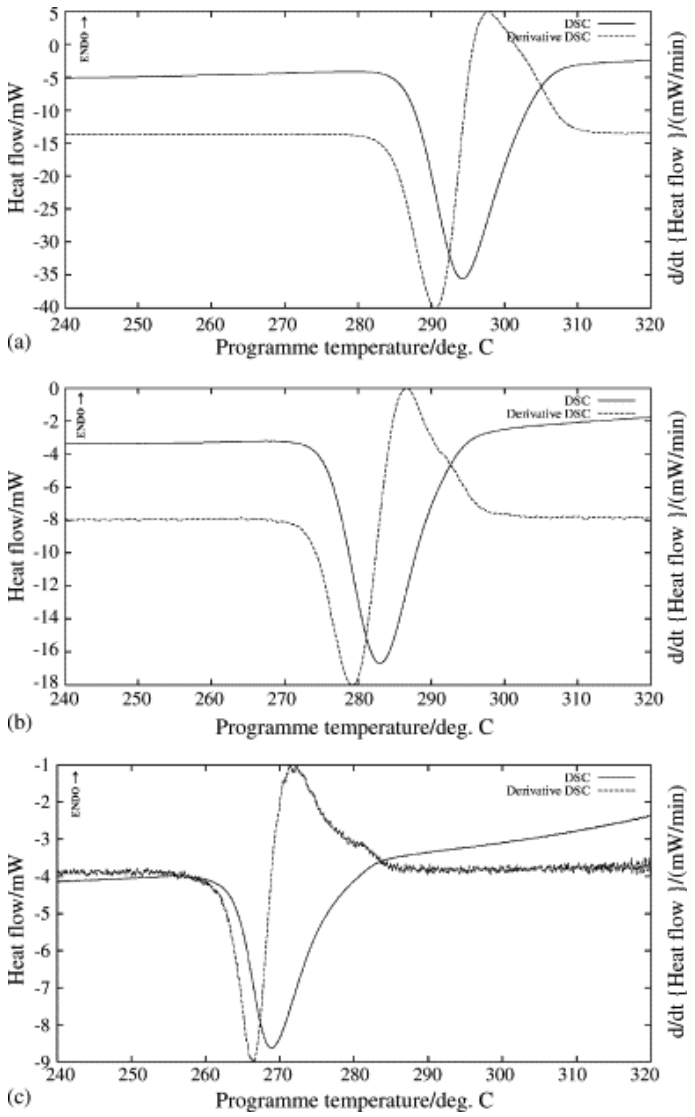

Fig. 9. DSC curves for copper(II) oxalate heated under nitrogen (25 mL min^{-1}) from 25 to 360 °C at: (a) 10 °C min^{-1}; (b) 5 °C min^{-1}; (c) 2 °C min^{-1}.

Table 4 is a summary of the DSC results at different heating rates under argon and nitrogen. It is clear that slower heating rates give rise to greater oxidation of the residues under both argon and nitrogen.

Table 4.

DSC results for copper(II) oxalate heated at various heating rates in crimped aluminium pans under argon and under nitrogen atmospheres (24 ± 1 mL min^{-1})

Heating rate (°C min^{-1})	100% Argon			100% Nitrogen		
	10	5	2	10	5	2
Residual mass (%)	42.38	42.68	44.08	42.20	42.62	44.05
Q (J g^{-1})	263	254	224	−435	−385	−331
$\Delta_r H$ (kJ mol^{-1})	40.0	38.5	34.0	−66.1	−58.5	−50.2

Although the data appear to suggest that more of both copper(I) oxide (cuprite) and copper(II) oxide (tenorite) are formed at 2 than at 5 °C min^{-1}, these conclusions are semi-quantitative at best and the proportions of each cannot be estimated with any accuracy from the X-ray powder diffraction and mass data.

The greater relative masses of the residues (i.e. $100m_r/m_s$) at 2 °C min^{-1} under both argon and nitrogen cannot reasonably be attributed to oxidation by residual air in the DSC furnace. Preliminary purging was extensive and the longer runtimes associated with slower heating rates would further decrease the effects of any such contamination. Even under the unreasonable assumption that all the oxygen impurity in the purge gas (2–3 vpm) reacts with the sample during the total run time, it can be calculated that this is not enough to account for the observed mass increase. This mass increase is thus probably due to greater oxidation of the sample material during decomposition by reaction with carbon dioxide. Mohamed et al., report similar relative residue masses of around 44% under nitrogen and carbon-dioxide atmospheres [6] at various heating rates.

3.6. DSC results at various purge gas flow-rates

Fig. 10 and Fig. 11 show DSC curves of copper(II) oxalate heated 10 °C min^{-1} under argon and nitrogen, respectively, at various flow rates. Table 5 summarizes the DSC results.

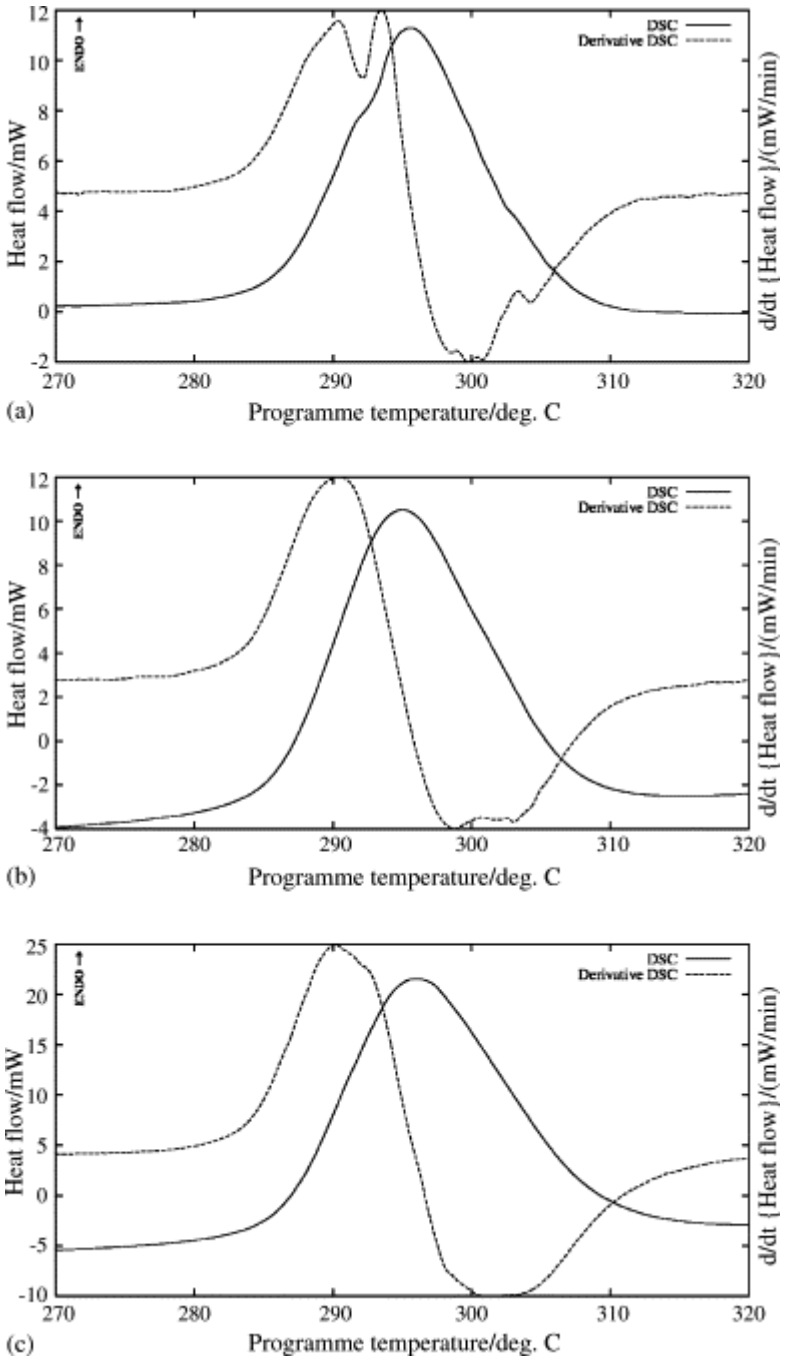

Fig. 10. DSC curves for copper(II) oxalate heated under argon from 25 to 360 °C at 10 °C min^{-1} at various flow rates: (a) 33 mL min^{-1}; (b) 25 mL min^{-1}; (c) 17 mL min^{-1}.

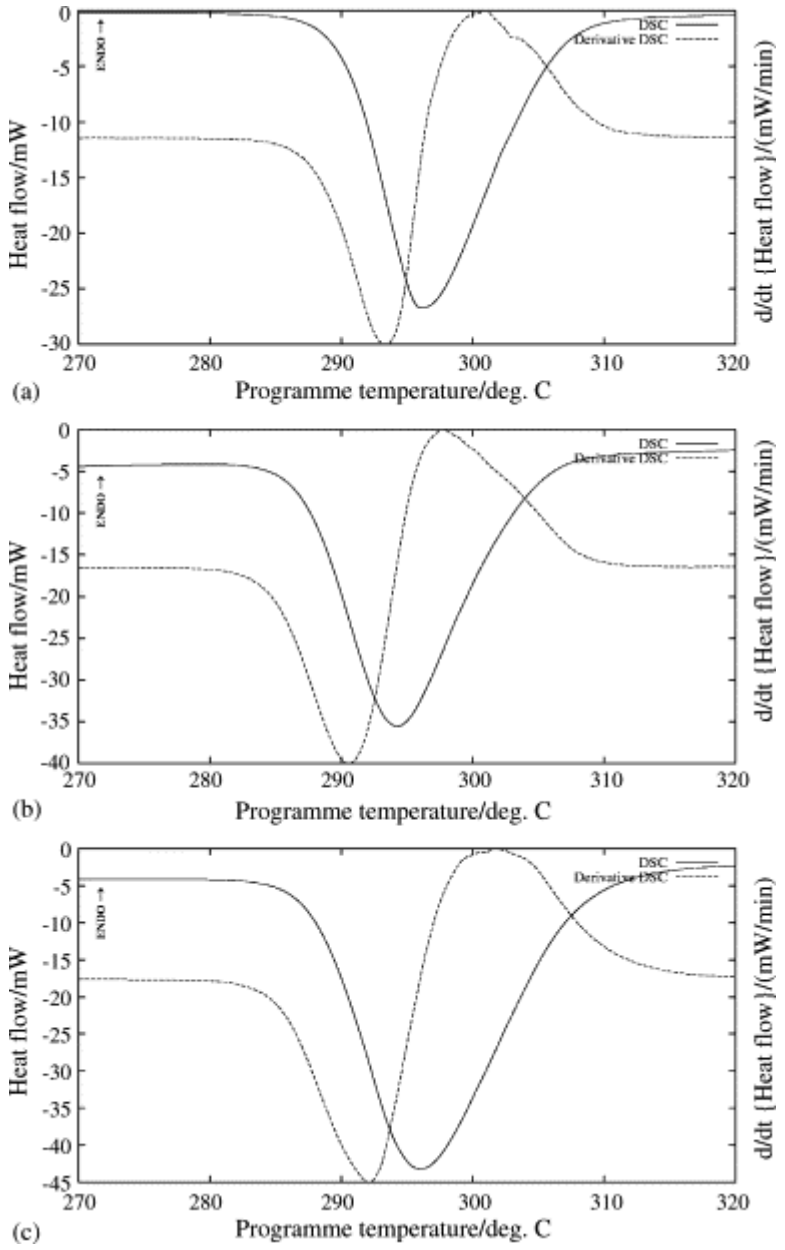

Fig. 11. DSC curves for copper(II) oxalate heated under nitrogen from 25 to 360 °C at 10 °C min^{-1} at various flow rates: (a) 30 mL min^{-1}; (b) 24 mL min^{-1}; (c) 15 mL min^{-1}.

Table 5.

DSC results for copper(II) oxalate heated at 10 °C min^{-1} at various flow rates in crimped aluminium pans under argon and under nitrogen atmospheres

Flow rate (mL min^{-1})	100% Argon			100% Nitrogen		
	33	25	17	30	24	15
Residual mass (%)	41.84	42.38	42.47	41.87	42.20	42.41
Q (J g^{-1})	187	263	489	−397	−435	−749
$\Delta_r H$ (kJ mol^{-1})	28.4	40.0	74.3	−60.4	−66.1	−114

Under both argon and nitrogen, decreasing the flow-rate of the purge gas results in peak broadening and loss of resolution. Very small increases in relative residue mass are observed under both argon and nitrogen as the purge-rates are decreased, which are also inconsistent with oxidation by oxygen contamination in the purge gases. The absolute values of $\Delta_r H°$ under both argon and nitrogen, as estimated by integrating the DSC curves, appear to depend very much on the purge gas flow rate.

$\Delta_r H°$ approximately doubles as the flow-rates are approximately halved. This behaviour does not agree with what is observed with the standard calibrant (indium metal).

The X-ray diffraction patterns under argon and nitrogen show that all of the DSC residues consist of mixtures of copper metal and copper(I) oxide (cuprite), with no copper(II) oxide (tenorite) observed. In agreement with the mass data, the X-ray diffraction patterns suggest that, under both argon and nitrogen atmospheres, the relative amount of copper(I) oxide in the DSC residues increases as the purge gas flow-rate is decreased.

4. Discussion

The fact the thermal decomposition of copper(II) oxalate is exothermic in atmospheres often regarded as inert, such as nitrogen and carbon dioxide, and in hydrogen, a reducing atmosphere, but appears to be endothermic in argon, suggests that a different reaction is taking place under argon. However, all other observations made in this study suggest that the reactions under nitrogen and under argon are the same. X-ray diffraction studies of residues from DSC experiments under argon and nitrogen show that these are very similar, and no significant difference could be observed by mass measurements of the DSC residues or by thermogravimetry. TG-FT-IR evidence suggests that practically the same gaseous products are released during decomposition under argon and nitrogen.

In nitrogen, the possible formation of copper nitride has to be considered. Cu_3N exists [9] and decomposition temperatures reported in the literature vary widely. The most reliable reports, which show DSC curves in specified atmospheres, record exothermic decomposition at temperatures greater than 327 °C under nitrogen [21], and at approximately 350 °C under argon [22]. The X-ray diffraction pattern [23] of copper nitride is distinguishable from those of copper metal and the copper oxides. However, there was no evidence from XRPD patterns of the DSC residues, obtained in this study, of the presence of copper nitride, so any participation by copper nitride in the thermal decomposition of copper(II) oxalate in nitrogen would have to be temporary, and thermochemical contributions to the formation and subsequent decomposition of copper nitride as an intermediate would cancel out. Exothermic decomposition is also not exclusive to nitrogen, but occurs under CO_2 and H_2 atmospheres as well.

Oxidation by impurities in the purge gases of the DSC is unlikely because of the similarity of the impurity specifications for argon and nitrogen and because preliminary DSC studies with a 15 ppb oxygen trap showed the same behaviour as without the trap.

For all the DSC runs in which the sample was heated at 10 °C min^{-1}, the residues were identified by X-ray powder diffraction as mainly copper metal with a small amount of copper(I) oxide (cuprite). Carbon monoxide gas was detected in the gas evolved during TG-experiments, so the DSC response could be described by Eq. (9):

$$\Delta_r H°(\beta)\ (\text{kJ mol}^{-1}) = 58.13\beta - 35.56 \qquad (9)$$

For the overall DSC response to be endothermic would require $\beta > 0.6117$ and Eq. (8) becomes:

$$CuC_2O_4(s) \rightarrow 0.3883Cu(s) + 0.3059Cu_2O(s) + 0.3059CO(g) + 1.6942CO_2(g)$$

and the calculated residual mass should be 45.06% of the original sample mass. This is significantly different from the experimental value of approximately 42% obtained for the various DSC runs at 10 °C min^{-1}.

The reasoning above may be reinforced by removing any dependence in the thermochemical calculations on the value of $\Delta_f H°CuC_2O_4(s)$ by defining β_{endo} as the value of β at the experimental endothermic response of 46.68 kJ mol^{-1} and β_{exo}, similarly, at the experimental exothermic response of −63.00 kJ mol^{-1}, then:

$$\beta_{endo} - \beta_{exo} = 1.883$$

which is not possible, because $0 \leq \beta \leq 1$. The mechanism is therefore not consistent with the observed experimental results, and cannot satisfactorily explain the endothermic DSC response under argon.

The DSC results at 5 and 2 °C min^{-1} are more difficult to interpret because of the additional formation of copper(II) oxide (tenorite) under both argon and nitrogen atmospheres at these heating rates. Everything else being unchanged, the effect of copper(II) oxide formation, at the expense of carbon dioxide formation, would be to render the DSC response more endothermic. The mass data and the X-ray powder diffraction patterns of the residues at different heating rates give no indication that the DSC residues under argon are different to those under nitrogen, and yet very different DSC responses are observed.

The DSC runs at different purge flow rates show that the DSC responses are strongly dependent on the purge rate. Under both argon and nitrogen purge, small increases in mass percentages of the residue are observed as the purge rate is decreased. XRPD of the residues show that only copper metal and copper(I) oxide are present, so oxidation of the solid residue at the expense of carbon dioxide production cannot satisfactorily explain the observed thermal behaviour.

A mismatch in thermal conductivity between the evolved gaseous products and the DSC purge gas can lead to spurious results. Hallbrucker and Mayer [24] used helium (50 mL min^{-1}) as a purge gas in a study of the thermal decomposition of large samples of copper(II) sulfate pentahydrate and found that spurious exotherms accompanied the evolution of water vapour. This was because of the large difference between the thermal conductivities of water vapour and of helium. They also reported similar behaviour under helium purge with samples known to evolve nitrogen gas. It would appear that the evolution of a gas with a significantly lower thermal conductivity than the instrument purge gas has the effect of blanketing the sample, thus reducing the heat flow from the sample furnace to the atmosphere compared to that of the reference furnace. The thermal conductivity of argon is a slightly closer match to that of carbon dioxide, the expected major evolved gas component in this study, than is the thermal conductivity of nitrogen, but the differences are small compared with the thermal conductivities of helium and hydrogen.

As mentioned in Section 1, kinetic arguments have been used to propose that the decompositions of silver(I), nickel(II) and mercury(II) oxalates are accompanied by the evolution of CO(g), CO_2(g) and (1/2)O_2(g) (or O), and that the oxalates of lead(II) and manganese(II) decompose to give CO(g) and (1/2)O_2(g) [11]. They are said to decompose by a mechanism of dissociative evaporation, i.e. by the congruent gasification of all reaction products irrespective of their saturated vapour pressure, with subsequent condensation of low-volatility species. Considering only the fraction of the available carbon dioxide, ω, which is released as CO(g) and either (1/2)O_2(g) or O(g):

$$CuC_2O_4(s) \rightarrow (1-\beta-\gamma)Cu(s) + (1/2)\beta Cu_2O(s) + \gamma CuO(s) + [(1/2)\beta + \gamma + \omega(2-(1/2)\beta-\gamma)]$$
$$CO(g) + (1-\omega)(2-(1/2)\beta-\gamma)CO_2(g) + [\omega(2-(1/2)\beta-\gamma)/2]O_2(g)$$

or

$$CuC_2O_4(s) \rightarrow (1-\beta-\gamma)Cu(s) + (1/2)\beta Cu_2O(s) + \gamma CuO(s) + [(1/2)\beta + \gamma + \omega(2-(1/2)\beta-\gamma)]$$
$$CO(g) + (1-\omega)(2-(1/2)\beta-\gamma)CO_2(g) + \omega(2-(1/2)\beta-\gamma)O(g)$$

if the oxygen is assumed to be monatomic. To simplify the problem, only mechanisms which do not involve the formation of copper(II) oxide will be considered (i.e. with $\gamma = 0$). Substituting the standard enthalpies of formation gives the numerical expressions:

$$\Delta_r H°(\beta, \omega) \text{ (kJ mol}^{-1}) = 58.13\beta + 565.83\omega - 141.46\beta\omega - 35.56$$

or

$$\Delta_r H°(\beta, \omega) \text{ (kJ mol}^{-1}) = 58.13\beta + 1064.14\omega - 266.04\beta\omega - 35.56$$

The sensitivity of these equations to the parameter, ω, is much greater than their sensitivity to β, so if a relatively small proportion of the available carbon dioxide were released as CO(g) and O_2(g), or as CO(g) and O(g), it would have a great effect on the observed heat flow, causing it to be more endothermic.

Fig. 12 illustrates the dependence of $\Delta_r H°(\beta, \omega)$ on β and ω for these mechanisms. Changes in ω have a much greater effect than changes in β on whether the reaction will be endothermic or exothermic. From the equations it can be seen that the amounts (and hence the masses) of the solid residues are not functions of ω. These mechanisms could thus explain the endothermic DSC responses, but many of the exothermic DSC responses in this study yield negative values considerably greater than -35.56 kJ mol^{-1} (the minimum value of the functions above). The exothermic DSC responses under nitrogen reported in the literature in recent years are by no means uniform as shown in Table 6. In addition, the ranges of the functions above are heavily dependent on the accuracy of the value for $\Delta_f H°CuC_2O_4$(s).

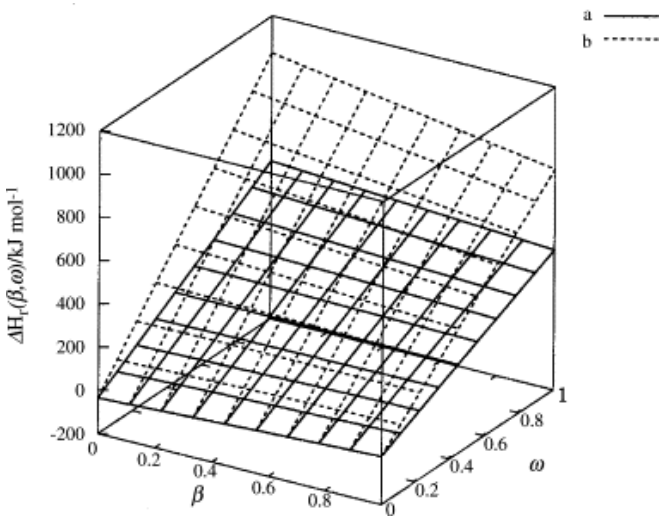

Fig. 12. The dependence of $\Delta_r H°(\beta, \omega)$ on β and ω for the proposed mechanisms involving the loss of (1/2)O_2(g) (surface a) and O(g) (surface b), showing the marked sensitivity to ω, the fraction of available CO_2 that is given off as CO and (1/2)O_2(g) or O (g).

Table 6.

Published DSC results for the thermal decomposition of copper(II) oxalate in different atmospheres and at various heating rates compared with the results obtained in this study

Atmosphere	Sample mass (mg)	Heating rate (°C min^{-1})	$\Delta_r H$ (kJ mol^{-1})	Reference
Argon (sealed ampoules)	28–32	2	−29 ± 2	[5]
Argon (33 mL min^{-1})	4	10	28	This
Nitrogen (30 mL min^{-1})	4–10	5	−9 ± 2	[27]
Nitrogen (40 mL min^{-1})	10–15	5	−11.9	[6]
Nitrogen (30 mL min^{-1})	4	10	−60	This
Air (30 mL min^{-1})	4–10	5	−134 ± 5	[27]
Air (40 mL min^{-1})	10–15	5 and 10	−18.0	[6]
Oxygen	1–5	20	−138 ± 4	[3]
Oxygen (36 mL min^{-1})	4	10	−224	This
Carbon dioxide (40 mL min^{-1})	10–15	5	−43.5	[6]
Hydrogen (40 mL min^{-1})	10–15	5 and 10	−21.1	[6]

Published DSC/DTA results for the decomposition of copper(II) oxalate at different heating rates and under various atmospheres are compared in Table 6 with the results obtained in this study. The largest value of $\Delta_r H°$ under nitrogen (i.e. that obtained in this study) is nearly six times the smallest. There is also little agreement between the DSC results under oxygen. The calculated enthalpy of the oxidation, using standard enthalpies of formation for CuO(s) and CO_2(g) [9] and a published value [10] of −751.3 kJ mol^{-1} for $\Delta_f H°CuC_2O_4$(s) is −190.6 kJ mol^{-1}. An experimental value close to this calculated value was obtained in this study.

The decompositions of copper(II) formate, acetate, malonate, fumarate and maleate take place [4] by complex mechanisms involving the formation of volatile and unstable copper(I) intermediates that cause copper to be deposited on the container walls. There is also evidence for the decomposition of copper(II) oxalate under vacuum proceeding via a copper(I) intermediate [25]. In this study, although the complexity of the DSC responses is consistent with a multi-step process, no evidence of copper deposition on the sample containers was observed.

5. Conclusions

The mechanism of thermal decomposition of copper(II) carboxylates is by no means resolved. The unexpected endothermic decomposition of copper(II) oxalate under argon cannot be explained unequivocally by the thermal, spectroscopic and X-ray methods employed in this study. The formation of oxygen gas or monatomic oxygen (in line with the proposal of L'vov [11]) may provide an explanation for the thermal behaviour. Similar atmosphere-dependent results have been found for more complex copper(II) compounds [1] and potential catalytic surfaces have been shown to give spurious DSC results for the decomposition of zinc, nickel and iron(II) oxalates in air [26]. As commented by a referee, the possibility exists that the exothermicity in nitrogen could be explained by reaction of the nitrogen with atomic oxygen to form N_2O(g), but this product could not be detected using TG-FT-IR.

References

[1] E. Lamprecht, G.M. Watkins, M.E. Brown, submitted for publication.

[2] D. Dollimore and D.L. Griffiths, *J. Therm. Anal.* 2 (1970), pp. 229–250

[3] A. Coetzee, D.J. Eve and M.E. Brown, *J. Therm. Anal.* 39 (1993), pp. 947–973.

[4] A.K. Galwey and M.E. Brown, Thermal Decomposition of Ionic Solids, Elsevier Science, Amsterdam (1999).

[5] E.A. Gusev, S.V. Dalidovich, V.A. Shandakov and A.A. Vecher, *Thermochim. Acta* 89 (1985), pp. 391–394.

[6] M.A. Mohamed, A.K. Galwey and S.A. Halawy, *Thermochim. Acta* 429 (2005), pp. 57–72.

[7] D. Dollimore, D.L. Griffiths and D. Nicholson, *J. Chem. Soc.* (1963), pp. 2617–2623.

[8] D. Dollimore, *Thermochim. Acta* 117 (1987), pp. 331–363.

[9] In: R.C. Weast, Editor, *CRC Handbook of Chemistry and Physics* (49th ed.), The Chemical Rubber Co., Cleveland, Ohio, USA (1968-1969).

[10] M.L. Van, *C.R.S. Acad. Sci. Ser. C Sci. Chim.* 272 (1971), pp. 2141–2143 (abstract CAN 76:7359).

[11] B.V. L'vov, *Thermochim. Acta* 364 (2000), pp. 99–109.

[12] B.V. L'vov, *Zh. Anal. Khim.* 45 (1990), pp. 2144–2153 (abstract CAN 114:50400).

[13] B.V. L'vov, *Mikrokhim. Acta* 2 (1991), pp. 299–308 (abstract CAN 115:288246).

[14] B.V. L'vov and A.V. Novichikhin, *Spectrochim. Acta B* 50 (1995), pp. 1427–1448.

[15] B.V. L'vov and A.V. Novichikhin, *Spectrochim. Acta B* 50 (1995), pp. 1459–1468.

[16] M.E. Brown, A.K. Galwey and M. Le Patourel, *Proceedings of the Sixth International Conference on Thermal Analysis, Bayreuth, Germany, July 1980, vol. 2* Birkhauser Verlag, Basel (1980), pp. 153–158.

[17] C.N. Banwell, Fundamentals of Molecular Spectroscopy (2nd ed.), McGraw-Hill, Maidenhead (1972).

[18] J. Mullens, A. Vos, R. Carleer, J. Ypemlan and L.C.V. Poucke, *Thermochim. Acta* 207 (1992), pp. 337–339.

[19] PerkinElmer Life and Analytical Sciences, TG/IR Interface, URL: http://www.las.perkinelmer:com/, part no. L1200502/L1200503.

[20] J.H. Slaghuis and P.M. Morgan, *Thermochim. Acta* 175 (1991), pp. 135–140.

[21] A. Baiker and M. Maciejewski, *J. Chem. Soc. Faraday Trans.* 1 (1983) (80), pp. 2331–2341.

[22] T. Nosaka, M. Yoshitake, A. Okamoto, S. Ogawa and Y. Nakayama, *Appl. Surf. Sci.* 169–170 (2001), pp. 358–361.

[23] J.F. Pierson, *Vacuum* 66 (2002), pp. 59–64.

[24] A. Hallbrucker and E. Mayer, *J. Therm. Anal.* 35 (1989), pp. 1733–1736.

[25] M.A. Mohamed and A.K. Galwey, *Thermochim. Acta* 217 (1993), pp. 263–276.

[26] R. Majumdar, P. Sarkar, U. Ray and M.R. Mukhopadhyay, *Thermochim. Acta* 335 (1999), pp. 43–53.

[27] D. Broadbent, J. Dollimore, D. Dollimore and T.A. Evans, *J. Chem. Soc., Faraday Trans. I* 87 (1991), pp. 161–166.